Photoemission and x-ray absorption study of misfit-layered (Bi,Pb)-Sr-Co-O compounds: Electronic structure of a hole-doped Co-O triangular lattice

T. Mizokawa*, L. H. Tjeng, and P. G. Steeneken
Solid State Physics Laboratory, Materials Science Centre, University of Groningen, Nijenborgh 4, 9747 AG Groningen, The Netherlands

N. B. Brookes
European Synchrotron Radiation Facility, BP 220, 38043, Grenoble, France

I. Tsukada**, T. Yamamoto, and K. Uchinokura
Department of Applied Physics and Department of Advanced Materials, University of Tokyo, Hongo 7-3-1, Bunkyo-ku, Tokyo 113-0033, Japan

(January 25, 2001)

We present a photoemission and x-ray absorption study of the misfit-layered (Bi,Pb)-Sr-Co-O compounds which have a Co-O triangular lattice with a mixed valence of Co^{3+} and Co^{4+}. The valence-band photoemission as well as the O 1*s* and Co 2*p* x-ray absorption spectra indicate that Co^{3+} and Co^{4+} have the low-spin t_{2g}^6 and t_{2g}^5 configurations, respectively. The angle-resolved photoemission spectra show that the dispersion of the t_{2g} feature is very small compared to its width at each angle, suggesting that the electron-lattice coupling energy is much larger than the kinetic energy of the t_{2g} electrons and that the carriers in the Co-O triangular lattice are essentially polarons formed by Co^{4+} in the nonmagnetic Co^{3+} background.

I. INTRODUCTION

Physical properties of hole-doped 3*d* transition-metal oxides have attracted much attention since the discovery of high-T_c superconductivity in Cu oxides[1] and colossal magnetoresistance (CMR) in Mn oxides.[2] Insights gained about these Cu and Mn oxides have triggered renewed interest in other strongly correlated materials, especially those that also reveal intriguing properties like the mixed-valent Co oxides. (La,Sr)CoO_3, for example, shows an evolution from a non-magnetic insulator ($LaCo^{3+}O_3$) to a ferromagnetic metal ($SrCo^{4+}O_3$).[3,4] Theoretical[5] and experimental[6–8] studies strongly suggest that in the ferromagnetic (La,Sr)CoO_3, Co^{3+} and Co^{4+} have the intermediate-spin configurations of $t_{2g}^5e_g^1$ and $t_{2g}^4e_g^1$, respectively. In such a case, the e_g electrons are relatively itinerant and give a double-exchange interaction between the localized t_{2g} spins. In fact, the magnetization of (La,Sr)CoO_3 is as large as 2 μ_B/Co which is consistent with the intermediate-spin state.

A decade ago, one of the variations of the mixed-valent Co oxides, namely $Bi_2Sr_3Co_2O_9$, has been assigned to have the same structure as the $Bi_2Sr_2CaCu_2O_8$ superconductor.[9] Accordingly, the Pb-doped (Bi,Pb)-Si-Co-O compound has also been considered to have the same structure.[10] However, a recent structural study of Yamamoto *et al.*[11] has shown that the (Bi,Pb)-Sr-Co-O system (including the Pb-undoped Bi-Sr-Co-O) has a misfit-layered structure isomorphous to $[Bi_{0.87}SrO_2]_2[CoO_2]_{1.82}$ recently reported by Leligny *et al.*[12] They contain a two-dimensional CoO_2 triangular lattice (see Fig. 1) with Co^{3+} and Co^{4+} mixed valence. Interestingly, Tsukada *et al.* have found that the misfit-layered (Bi,Pb)-Sr-Co-O compound is a ferromagnetic metal below 4 K and shows a negative magnetoresistance.[13] The magnetization of the (Bi,Pb)-Sr-Co-O compound is only ∼0.1 μ_B/Co which is much smaller than that of (La,Sr)CoO_3.[13] The small magnetization in the (Bi,Pb)-Sr-Co-O system suggests that Co^{3+} and Co^{4+} are in the low-spin state. Therefore, the (Bi,Pb)-Sr-Co-O system would provide an opportunity to study the electronic structure of the Co^{4+}-like species in the low-spin (non-magnetic) Co^{3+} background. The electronic structure of the CoO_2 triangular lattice is interesting in the light of the large thermoelectric power found in the (Bi,Pb)-Sr-Co-O compounds[14,15], the $NaCo_2O_4$ compounds[16], and the $Ca_3Co_4O_9$ compounds,[17,18] all of which have the metallic CoO_2 triangular lattice in common as shown in Fig. 1.[19,20]

In this paper, we present a photoemission and x-ray absorption study of the misfit-layered Bi-Sr-Co-O and (Bi,Pb)-Sr-Co-O compounds and discuss the electronic structure of the hole-doped Co-O triangular lattice. We also make a comparison with the angle-resolved photoemission (ARPES) results from the layered CMR Mn oxide $(La,Sr)_3Mn_2O_7$,[21] and discuss the differences.

II. EXPERIMENTAL

Single crystals of the misfit-layerd Bi-Sr-Co-O and (Bi,Pb)-Sr-Co-O compounds were prepared by a floating zone method and consist of the $(Bi,Pb)SrO_2$ rock-salt layer and the CoO_2 hexagonal layer as reported in the literature.[11,13] The actual composition of the

Bi-Sr-Co-O and (Bi,Pb)-Sr-Co-O single crystals are $Bi_{2.0}Sr_{2.1}Co_{2.0}O_y$ and $Bi_{1.5}Pb_{0.5}Sr_{2.1}Co_{2.0}O_y$, respectively, which were measured by inductively coupled plasma atomic emission spectroscopy. Since the chemical composition of the Bi-Sr-Co-O compound is approximately given by $[Bi_{0.87}SrO_2]_2[CoO_2]_{1.82}$, the average valence of Co ions is expected to be +3.33.[12,13] For the (Bi,Pb)-Sr-Co-O case, by assuming that the oxygen content is not changed by the Pb doping, the average valence of Co ions is estimated to be +3.52.[13] While the in-plane resistivity of the Bi-Sr-Co-O sample increases at low temperature and exceeds 100 mΩ cm at 4 K, that of the (Bi,Pb)-Sr-Co-O sample is smaller than 10 mΩ cm at 4 K and shows a metallic behavior in almost whole temperature region.[13]

X-ray photoelectron spectroscopy (XPS) experiments were carried out in a Vacuum Generators (VG) Surface Science X-probe spectrometer unit, equipped with a small spot (150-1000 μm) Al-K_α source ($h\nu$=1486.6 eV) monochromatized by a VG twin-crystal monochromator, and with a hemispherical electron energy analyzer with multichannel detection system. The XPS overall energy resolution was 0.5 eV, as determined using the Fermi cut-off of a Ag reference sample. The zero of the binding energy scale was given by the Fermi level of this Ag reference. ARPES measurements were done using a VG He discharge lamp and a VG hemispherical electron analyzer installed on a two-axis goniometer. The acceptance angle of the analyzer was 2° and the energy resolution was set to ~50 meV. X-ray absorption spectroscopy (XAS) were performed using the helical undulator beamline ID12B of the European Synchrotron Radiation Facility in Grenoble.[22,23] The degree of circular polarization was ~92%. For the XPS, ARPES, and XAS measurements, the samples were cleaved *in situ* under ultra high vacuum conditions of low 10^{-10} Torr. All the spectra were taken at room temperature. The cleanliness of the surfaces was checked by the lack of the contamination/degradation-related feature on the higher binding energy side in the O 1*s* XPS spectra and the feature at ~9.5 eV in the ARPES spectra.

III. RESULTS AND DISCUSSION

A. XPS

Figure 2 shows the O 1*s* core-level XPS spectra of the Bi-Sr-Co-O and (Bi,Pb)-Sr-Co-O samples. The difference between the O 1*s* binding energies is less than 0.1 eV. In the (La,Sr)CoO_3 system, the O 1*s* binding energy is lowered by ~0.4 eV in going from $LaCoO_3$ to $La_{0.8}Sr_{0.2}CoO_3$ and by ~0.1 eV in going from $La_{0.8}Sr_{0.2}CoO_3$ to $La_{0.4}Sr_{0.6}CoO_3$.[8] The binding energy shift of ~0.4 eV between $LaCoO_3$ and $La_{0.8}Sr_{0.2}CoO_3$ is attributed to the shift of the chemical potential across the band gap of $LaCoO_3$.[8] The binding energy shift between the Bi-Sr-Co-O and (Bi,Pb)-Sr-Co-O compounds is small because the Bi-Sr-Co-O sample is already hole-doped and the chemical potential is pinned near the top of the valence band in both compounds. This picture is also supported by the valence-band spectra presented in the following paragraphs. The lack of the contamination/degradation-related feature, which is expected at ~532 eV,[8] indicates the good quality of the surface.

The Co 2*p* XPS spectra are shown in Fig. 3. The binding energy of the Co $2p_{3/2}$ main peak is ~779.0 eV. The charge-transfer satellite of the Co $2p_{3/2}$ peak is located at ~789.0 eV. The satellite structure for the Co $2p_{1/2}$ peak is overlaid with the Bi $4p_{1/2}$ peak. The energy difference between the main and satellite peaks is ~10 eV in the Bi-Sr-Co-O and (Bi,Pb)-Sr-Co-O compounds, which is approximately the same as that in (La,Sr)CoO_3.[8] Therefore, the electronic-structure parameters such as the charge-transfer energy are expected to be similar to those for (La,Sr)CoO_3.

The valence-band XPS spectra are shown in Fig. 4 which are normalized using the intensity at ~14 eV. Structure A, which is derived from the Co t_{2g} states, is located at ~1 eV. The intensity of structure A is reduced in going from Bi-Sr-Co-O to (Bi,Pb)-Sr-Co-O, which is consistent with the fact that the Pb-substitution introduces extra holes in the t_{2g} states.[13] Structures B, C, and D are mainly constructed from the O 2*p* state of the CoO_2 layer and the (Bi,Pb)SrO_2 rock-salt layer. As shown later, the ARPES data indicates that structures C and D are derived from the (Bi,Pb)SrO_2 layer and that structure B originates from the CoO_2 layer. Although the Bi-Sr-Co-O and (Bi,Pb)-Sr-Co-O samples are expected to be hole-doped, the Co t_{2g} peak (structure A) is and remains sharp with a line shape very similar to that of $LiCoO_2$ and $LaCoO_3$ which have the low-spin t_{2g}^6 configuration.[24,25] Therefore, the photoemission spectra shown in Fig. 4 suggest that in the (Bi,Pb)-Sr-Co-O system the Co^{3+} state remains in the low-spin t_{2g}^6 configuration even when the material is heavily hole doped, and that the spectral weight near the Fermi level is dominated by the t_{2g} states. This situation is in contrast to (La,Sr)CoO_3 where the Co t_{2g} peak collapses rapidly with hole doping.[8] It is known that in (La,Sr)CoO_3 hole doping induces the transition of the low-spin states to the intermediate-spin states and that the e_g states are partially occupied near the Fermi level.[5,6] This transition is responsible for the rapid destruction of the t_{2g} peak and the formation of the broad e_g band near the Fermi level in (La,Sr)CoO_3.[8]

Yamamoto *et al.* have reported that the Pb doping reduces the *b*-axis length of the (Bi,Pb)SrO_2 rock-salt layer from 5.4 Åto 5.2 Å. The structural change induced by the Pb doping could influence the electronic structure of the (Bi,Pb)SrO_2 layer. For example, a reduction of the Bi(Pb)-O bond length due to Pb doping may enhance the hybridization between the O 2*p* and Bi(Pb) 6*s*/6*p* states. In fact, the intensity of structures C and D

from the (Bi,Pb)SrO_2 layer increases with the Pb doping, indicating that the O $2p$ states in the (Bi,Pb)SrO_2 layer are indeed affected by the Pb doping. The doping also shifts the Bi $6s$ and $4f$ peaks towards higher binding energies by ~0.3 eV.

B. XAS

Figure 5(a) shows the O $1s$ XAS spectra of Bi-Sr-Co-O and (Bi,Pb)-Sr-Co-O taken at normal ($\theta = 0°$) and off-normal ($\theta = 60°$) incidence. θ is the angle between the Poynting vector of the circularly polarized light and the z direction which is normal to the cleaved surface and the CoO_2 layer. Structures α and β are derived from the transitions from the O $1s$ core level to the O $2p$ states hybridized into the unoccupied Co t_{2g} and e_g states, respectively. This assignment is consistent with the O $1s$ XAS studies on $LaCoO_3$ and $LiCoO_2$.[25,26] The O $1s$ XAS spectra are normalized and aligned at structure β which would not be affected by the Pb doping if Co^{3+} and Co^{4+} have the low-spin configurations. Structure γ is the transition from O $1s$ to O $2p$ which is mixed into the unoccupied Bi and Pb $6p$ orbitals. The intensity of structure γ increases in going from Bi-Sr-Co-O to (Bi,Pb)-Sr-Co-O, indicating that the hybridization between the O $2p$ and Bi(Pb) $6p$ states is enhanced by the Pb doping. This would be consistent with the reduction of b-axis length induced by the Pb doping.[11]

As shown in Fig. 5(b), the intensity of structure α is dramatically enhanced in going from normal ($\theta = 0°$) to off-normal ($\theta = 60°$). In order to quantitatively analyze these data, we have fitted the O $1s$ XAS spectra using two Gaussians for structures α and β, and the tail of another Gaussian to represent the tail of structure γ. The results are plotted in Fig. 5(c), showing the good fit to the experimental data. The intensity ratio of structure α at $\theta = 60°$ to that at $\theta = 0°$ is thus estimated to be 2.4 and 2.1 for Bi-Sr-Co-O and (Bi,Pb)-Sr-Co-O, respectively. Theoretically, the intensity of O $1s$ XAS is determined by the dipole matrix element of the O $1s$-$2p$ transition. The transitions to the O $2p_x/2p_y$ and $2p_z$ orbitals have θ dependences of $\frac{1}{2} + \frac{1}{2}\cos^2\theta$ and $\frac{1}{2}\sin^2\theta$, respectively, for circularly polarized light. Under the trigonal crystal field, the three t_{2g} orbitals are split into a_{1g} orbital [$\frac{1}{\sqrt{3}}(|x'y'\rangle + |y'x'\rangle + |z'x'\rangle) = |3z^2 - r^2\rangle$] and the two e'_g orbitals [$\frac{1}{\sqrt{3}}(|x'y'\rangle + e^{\pm\frac{2\pi}{3}i}|y'x'\rangle + e^{\pm\frac{4\pi}{3}i}|z'x'\rangle)$], where the x', y', and z' axes are the three axes through the center and the corners of the CoO_6 octahedron. For the a_{1g} orbital, the transfer integral with $2p_z$ is $\frac{2}{3}(pd\pi)$ and the average transfer integral with $2p_x/2p_y$ is given by $\frac{1}{3}(pd\pi)$. For the e'_g orbitals, the average transfer integral with $2p_z$ is $\frac{1}{3}(pd\pi)$ and that with $2p_x/2p_y$ is $\frac{\sqrt{10}}{6}(pd\pi)$. Therefore, the intensity of structure α is expected to have the angle dependence of $\frac{1}{2}(\frac{2n_a+5n_e}{18})(\cos^2\theta + 1) + \frac{1}{2}(\frac{4n_a+n_e}{9})\sin^2\theta$. Here, n_a and n_e are the number of holes in the a_{1g} and e'_g states, respectively. For $n_a = 1$ and $n_e = 0$, the intensity ratio is calculated to be 2.1 which agrees well with the experimental value. On the other hand, the intensity ratio is 1.2 for $n_a = n_e = 1$ and is 0.8 for $n_a = 0$ and $n_e = 1$. Therefore, one can conclude that the holes are mainly located in the a_{1g} orbital. This situation is possible only when Co^{4+} has the low-spin t_{2g}^5 configuration (four electrons in e'_g and one electron in a_{1g}). The intensity of structure α is not changed in going from Bi-Sr-Co-O to (Bi,Pb)-Sr-Co-O although the additional holes are introduced by the Pb doping. However, since the Co-O distance and the strength of the Co-O hybridization might be changed by the Pb doping, the intensity of structure α does not necessarily reflect directly the hole concentration in the a_{1g} orbital. Another possibility is that the oxygen content is reduced by the Pb doping and, consequently, the number of holes in (Bi,Pb)-Sr-Co-O is close to that in Bi-Sr-Co-O.

Figure 6 shows the Co $2p$ (L_{23}) XAS spectra of the Bi-Sr-Co-O and (Bi,Pb)-Sr-Co-O samples taken at normal light incidence. The spectra are dominated by the $2p$ core-hole spin-orbit coupling, which splits the spectra roughly into two parts, namely the L_3 ($h\nu \sim 780$ eV) and L_2 ($h\nu \sim 795$ eV) white line regions, separated by about 15 eV. Since the effect of the core-hole potential is substantial in the Co $2p$ XAS spectra compared to that in the O $1s$ XAS spectra, the Co $2p$ XAS final states are well described by the multiplet structure due to the Coulomb and exchange interactions between the Co $2p$ core hole and the Co $3d$ electrons, the spin-orbit interactions, and the crystal-field splittings of the Co $3d$ subshell. The dipole selection rules make the spectra strongly to depend on the symmetry of the initial state of the Co ions. The rather large intensity ratio between the L_2 and L_3 structures (i.e. the L_2/L_3 branching ratio) indicates that the Co ions in both compounds mainly have a local low-spin state character.[27,28] In fact, the line shape of the Co $2p$ spectra (especially, in the L_2 region) are rather similar to the multiplet calculations starting from the low-spin ground states (the t_{2g}^6 configuration for the Co^{3+} ion[25] and the t_{2g}^5 configuration for the Co^{4+} ion[7]) and are very different from those for the intermediate-spin or high-spin ground states.

C. ARPES

ARPES data taken at $h\nu = 21.2$ eV are shown in Fig. 7. The ARPES data in the left panel were taken approximately along the ΓY direction of the (Bi,Pb)SrO_2 layer and is the Co-Co direction of the Co-O triangular lattice as indicated in Fig. 1. ARPES data along the ΓM direction of the (Bi,Pb)SrO_2 layer are shown in the right panel of Fig. 7. The band dispersion and the relative intensity of structures C and D are in good agreement with those reported for $Bi_2Sr_2CaCu_2O_8$,[29,30] indicating that structures C and D are derived from the surface (Bi,Pb)SrO_2

layer. On the other hand, there is no counterpart of structures A and B in $Bi_2Sr_2CaCu_2O_8$. Therefore, as discussed in the previous paragraph, structures A and B can be attributed to the Co t_{2g} and O $2p$ states of the CoO_2 layer. In order to show the dispersion of these features, the second derivatives of the ARPES spectra are shown in Fig. 8. While structure A is almost dispersionless, structures B, C and D have some dispersions, indicating that the observed spectrum at each angle is indeed angle-resolved. Therefore, we can conclude that the angle-independent t_{2g} feature is intrinsic to the hole-doped CoO_2 triangular lattice.

ARPES data near the Fermi level are plotted in Fig. 9. The t_{2g} spectral feature is centered at $\sim$0.9 eV and has the width of $\sim$1 eV. The width of the t_{2g} feature at each angle is very large compared to the dispersion of its centroid both in Bi-Sr-Co-O and in (Bi,Pb)-Sr-Co-O. At each angle, the tail of the t_{2g} feature reaches the Fermi level although the intensity at the Fermi level is considerably suppressed. As discussed in the previous paragraphs, the Bi-Sr-Co-O compound is already hole-doped and has the Fermi level near the top of the valence band. The line shape of the t_{2g} peak can be interpreted in terms of the single-electron excitation spectrum from the localized electron coupled with phonons.[31] In this picture, the centroid of the t_{2g} feature corresponds to the bare electron-removal excitation without lattice relaxations and the intensity at the Fermi level is derived from the final states fully stabilized by the lattice relaxation, namely, the final states with zero phonons.

It is interesting to compare the present ARPES data with that of $(La,Sr)_3Mn_2O_7$ reported by Dessau *et al.*[21] In $(La,Sr)_3Mn_2O_7$, although the ARPES features are broad and the spectral weight at the Fermi level is depleted, the centroid of the ARPES feature shows the substantial dispersion. Dessau *et al.* argue that the final state is dressed by phonon excitations ending up with the broad ARPES feature which can still have the large dispersion as predicted by the band structure calculation.[21] On the other hand, in the (Bi,Pb)-Sr-Co-O system, the band dispersion is negligibly small compared with the width of the spectral feature. The small band dispersion is reasonable because, in the CoO_2 triangular lattice, the Co-O-Co bond angle is close to 90° and the electron hopping term between the neighboring Co sites is expected to be small. In fact, a recent band-structure calculation for $NaCo_2O_4$ predicts that the t_{2g} band width is very narrow in the CoO_2 triangular lattice.[32] Probably, the difference between the square MnO_2 layer and the triangular CoO_2 layer originates from the difference between the metal-oxygen-metal bond angle as well as from the different involvement of the e_g and t_{2g} electrons. In the CoO_2 triangular lattice, the t_{2g} band width is small compared to the electron-lattice interaction term. Consequently, the effect of the electron-phonon coupling would be strong enough to form small polarons in the ground state.

It is also interesting that the line shape of the t_{2g} feature is not changed by hole doping as shown in Fig. 9. Probably, the coupling between the t_{2g} electrons and the optical phonons in the (Bi,Pb)-Sr-Co-O system is strong and does not depend on the hole concentration. This is also consistent with the picture that the Co^{4+} state induced by hole doping forms a kind of small polaron (Co^{4+} embedded in the nonmagnetic Co^{3+} background). Since spin and charge orderings are frustrated in the CoO_2 triangular lattice, the strongly-renormalized polaron band has more chance to survive at low temperature although the small polaron would be localized at very low temperature because of randomness. In future, relationships between the small polaron picture and the ferromagnetism and the enhanced thermoelectric power should be studied experimentally and theoretically.

IV. CONCLUSIONS

We have studied the electronic structure of misfit-layered (Bi,Pb)-Sr-Co-O compounds which have a Co-O triangular lattice with a mixed valence of Co^{3+} and Co^{4+}. The valence band XPS data shows that the t_{2g} peak remains sharp with hole doping, indicating that Co^{3+} has the low-spin t_{2g}^6 configuration and that the electronic states near the Fermi level are constructed from the t_{2g} states. The low spin configuration is also confirmed by the Co 2p XAS data. In addition, the O 1s XAS study reveals that the holes are mainly located in the a_{1g} orbital among the three t_{2g} orbitals and that Co^{4+} also has the low-spin t_{2g}^5 configuration. This situation is in sharp contrast to $(La,Sr)CoO_3$, in which Co^{3+} and Co^{4+} have the intermediate-spin configurations and the e_g electrons are involved in the electronic states near the Fermi level. Since the kinetic energy of the t_{2g} electrons are considerably small compared to that of the e_g electrons, the physical properties of (Bi,Pb)-Sr-Co-O are dominated by the electron-lattice interaction. In fact, the broad and angle-independent t_{2g} feature observed in ARPES is consistent with the single-electron excitation from the small and almost localized polarons.

ACKNOWLEDGEMENTS

The authors would like to thank K. Larsson and A. Heeres for skillful technical supports and I. Terasaki, D. I. Khomskii, C. Michel, B. Raveau and G. A. Sawatzky for valuable discussions. This work is supported by the Nederlands Organization for Fundamental Research on Matter (FOM) with final support from the Netherlands Organization for Scientific Research (NWO) and by the European Commission TRM network on Oxide Spin Electronics (OXSEN).

* Present address: Department of Complexity Science and Engineering, University of Tokyo.
** Present address: Central Research Institute of Electric Power Industry, 2-11-1 Iwado-kita, Komae-shi, Tokyo 201-8511, Japan.

[1] J. G. Bednorz, and K. A. Müller, Z. Phys. B **64**, 189 (1986).
[2] Y. Tokura, A. Urushibara, Y. Moritomo, T. Arima, A. Asamitsu, G. Kido, and N. Furukawa, J. Phys. Soc. Jpn. **63**, 3931 (1994); Y. Tokura, Y. Tomioka, H. Kuwahara, A. Asamitsu, Y. Moritomo, and M. Kasai, J. Appl. Phys. **79**, 5288 (1996).
[3] P. M. Raccah and J. B. Goodenough, Phys. Rev. **155**, 932 (1967)
[4] G. H. Jonker and J. H. van Santen, Physica **19**, 120 (1953).
[5] M. A. Korotin, S. Yu. Ezhov, I. V. Solovyev, V. I. Anisimov, D. I. Khomskii, and G. A. Sawatzky, Phys. Rev. B **54**, 5309 (1996).
[6] S. Yamaguchi, Y. Okimoto, H. Taniguchi, and Y. Tokura, Phys. Rev. B **53**, R2926 (1996).
[7] R. H. Potze, G. A. Sawatzky, and M. Abbate, Phys. Rev. B **51**, 11501 (1995).
[8] T. Saitoh, T. Mizokawa, A. Fujimori, M. Abbate, Y. Takeda, and M. Takano, Phys. Rev. B **56**, 1290 (1997).
[9] J. M. Tarascon, R. Ramesh, P. Barboux, M. S. Hedge, G. W. Hull, L. H. Green, M. Giroud, Y. LePage, W. R. McKinnon, J. W. Waszczak, and L. F. Schneemeyer, Solid State Commun. **71**, 663 (1989).
[10] I. Tsukada, T. Yamamoto, M. Takagi, T. Tsubone, and K. Uchinokura, Mat. Res. Soc. Symp. Proc. **494**, 119 (1998).
[11] T. Yamamoto, I. Tsukada, K. Uchinokura, M. Takagi, T. Tsubone, M. Ichihara, and K. Kobayashi, Jpn. J. Appl. Phys. **39**, L747 (2000).
[12] H. Leligny, D. Grebille, O. Pérez, A. Masset, M. Hervieu, C. Michel, and B. Raveau, C. R. Acad. Sci. Paris, Série II. **2**, 409 (1999).
[13] I. Tsukada, T. Yamamoto, M. Takagi, T. Tsubone, S. Konno K. Uchinokura, to be published in J. Phys. Soc. Jpn.
[14] R. Funahashi, I. Matsubara, and S. Sodeoka, Appl. Phys. Lett. **76** 2385 (2000).
[15] T. Itoh and I. Terasaki, submitted to J. Phys. Soc. Jpn.
[16] I. Terasaki, Y. Sasago, and K. Uchinokura, Phys. Rev. B **56**, R12685 (1997).
[17] A. C. Masset, C. Michel, A. Maignan, M. Hervieu, O. Toulemonde, F. Studer, B. Raveau, and J. Hejtmanek, Phys. Rev. B **62**, 166 (2000).
[18] Y. Miyazaki, K. Kudo, M. Akoshima, Y. Ono, Y. Koike, and T. Tajitani, Jpn. J. Appl. Phys. **39** L531 (2000).
[19] M. Jansen and R. Hoppe, Z. Anorg. Allg. Chem. **408**, 104 (1974).
[20] T. Tanaka, S. Nakamura, and S. Iida, Jpn. J. Appl. Phys. **33**, L581 (1994)
[21] D. S. Dessau, T. Saitoh, C.-H. Park, Z.-X. Shen, P. Villella, N. Hamada, Y. Moritomo, and Y. Tokura, Phys. Rev. Lett. **81**, 192 (1998).
[22] P. Elleaume, J. Synchrotron Radiat. **1**, 19 (1994).
[23] J. Goulon *et al.*, Physica (Amsterdam) **208B**, 199 (1995).
[24] J. van Elp, J. L. Wieland, H. Eskes, P. Kuiper, G. A. Sawatzky, F. M. F. de Groot, and T. S. Turner, Phys. Rev. B **44**, 6090 (1991).
[25] M. Abbate, J. C. Fuggle, A. Fujimori, L. H. Tjeng, C. T. Chen, R. Potze, G. A. Sawatzky, H. Eisaki, S. Uchida, Phys. Rev. B **47** 16124 (1993).
[26] F. M. F. de Groot, M. Abbate, J. van Elp, G. A. Sawatzky, Y. J. Ma, C. T. Chen, and F. Sette, J. Phys. Condens. Matter **5**, 2277 (1993).
[27] G. van der Laan, B. T. Thole, G. A. Sawatzky, M. Verdaguer, Phys. Rev. B **37**, 6587 (1988).
[28] C. Cartier dit Moulin, P. Rudolf, A.-M. Flank, C. T. Chen, J. Phys. Chem. **96**, 6196 (1992).
[29] P. A. P. Lindberg, Z.-X. Shen, D. S. Dessau, B. O. Wells, D. B. Mitzi, I. Lindau, W. E. Spicer, and A. Kapitulnik, Phys. Rev. B **40**, 5169 (1989).
[30] T. Takahashi, H. Matsuyama, H. Katayama-Yoshida, Y. Okabe, S. Hosoya, K. Seki, H. Fujimoto, M. Sato, and H. Inokuchi, Phys. Rev. B **39**, 6636 (1989).
[31] G. D. Mahan, *Many Particle Physics*, (Plenum Press, New York, 1990), Chap. 4.
[32] D. J. Singh, Phys. Rev. B **61**, 13397 (2000).

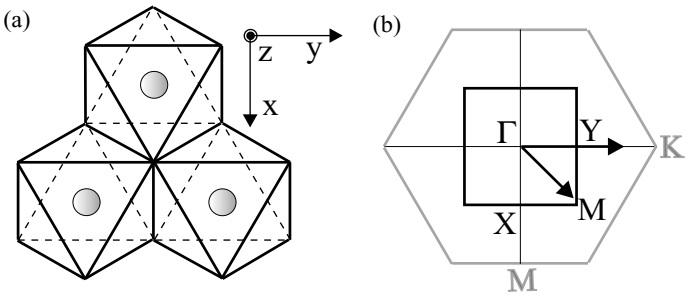

FIG. 1. (a) A schematic picture of the CoO_2 triangular lattice. The shaded circles indicate Co ions centered at the CoO_6 octahedra sharing their edges. (b) The first Brillouin zone of the (Bi,Pb)SrO_2 rock-salt layer (thick solid line) and that of the hexagonal CoO_2 layer (thick gray line). For the (Bi,Pb)SrO_2 layer, the Γ, X, Y, and M points are shown. For the hexagonal CoO_2 layer, the K and M points are indicated by the gray letters. The arrows indicate the ΓY, and ΓM directions of the (Bi,Pb)SrO_2 rock-salt layer along which the ARPES data were taken.

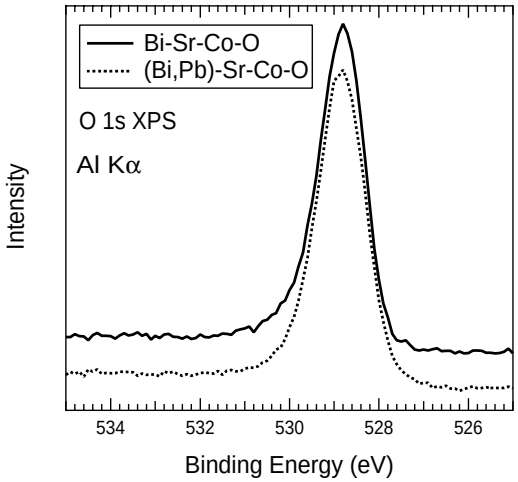

FIG. 2. O 1*s* core-level XPS spectra of the Bi-Sr-Co-O and (Bi,Pb)-Sr-Co-O samples.

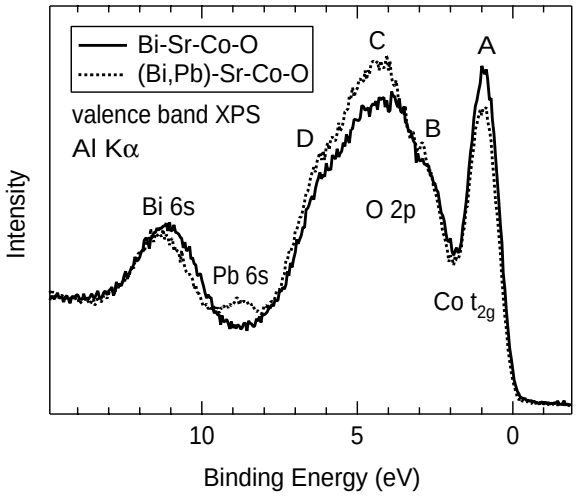

FIG. 4. Valene-band XPS spectra of the Bi-Sr-Co-O and (Bi,Pb)-Sr-Co-O samples.

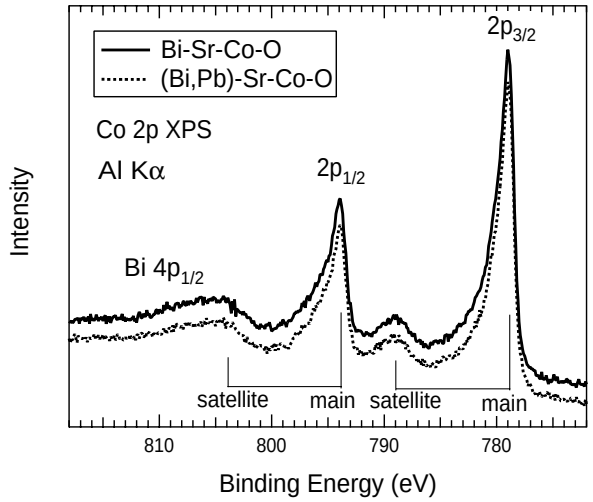

FIG. 3. Co 2*p* core-level XPS spectra of the Bi-Sr-Co-O and (Bi,Pb)-Sr-Co-O samples.

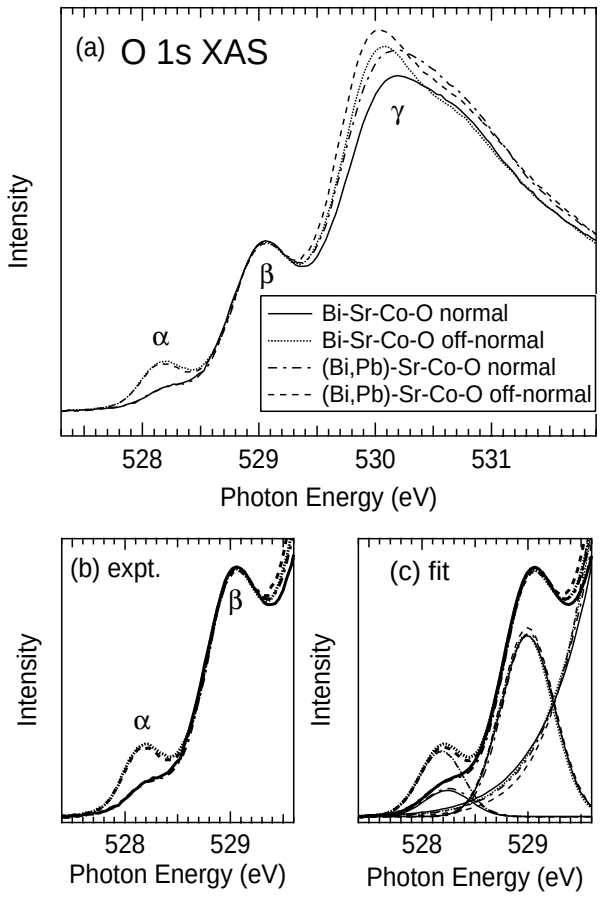

FIG. 5. (a) and (b) O 1s XAS spectra of the Bi-Sr-Co-O and (Bi,Pb)-Sr-Co-O samples taken at normal ($\theta = 0°$) and off-normal ($\theta = 60°$) incidence. θ is the angle between the Poynting vector of the circularly polarized light and the z direction which is normal to the CoO_2 layer. The spectra are normalized and aligned at structure β. (c) Fitted results (thick curves) for the O 1s XAS spectra using two Gaussians for structures α and β, and the tail of another Gaussian to represent the tail of structure γ. The thin curves indicate the Gaussian for structure α, that for structure β, and the tail of structure γ.

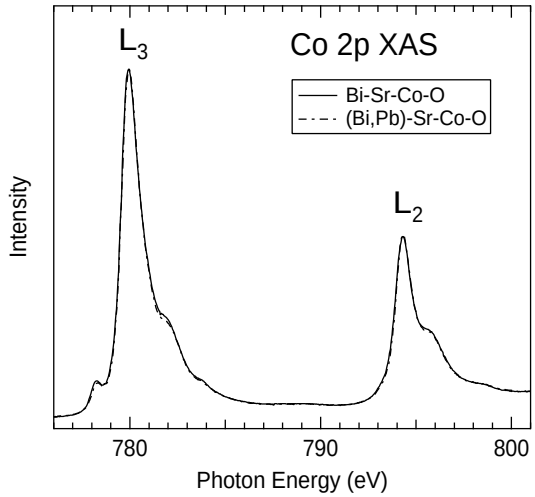

FIG. 6. Co 2p (L_{23}) XAS spectra of the Bi-Sr-Co-O and (Bi,Pb)-Sr-Co-O samples taken at normal light incidence.

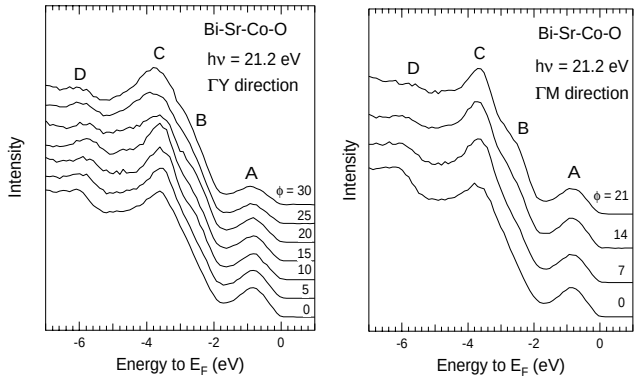

FIG. 7. ARPES spectra of the Bi-Sr-Co-O sample along the ΓY and ΓM directions of the (Bi,Pb)SrO_2 layer. ϕ denotes an angle between the sample surface normal and the emission direction of the collected photoelectrons.

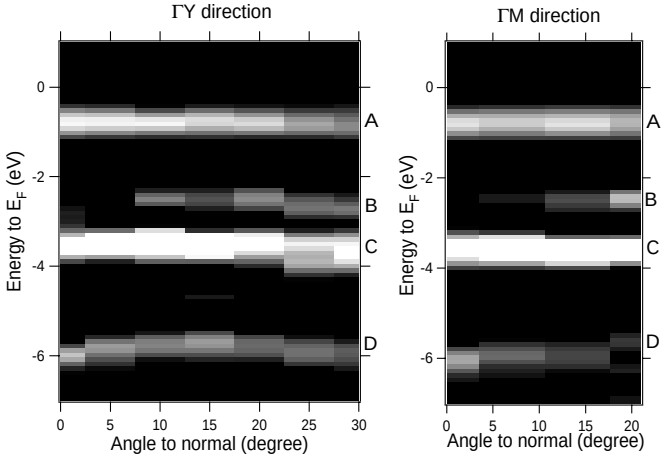

FIG. 8. Second derivatives of the ARPES spectra of the Bi-Sr-Co-O sample along the ΓY and ΓM directions of the (Bi,Pb)SrO_2 layer. The bright regions labeled as A, B, C, and D correspond to the dispersive features.

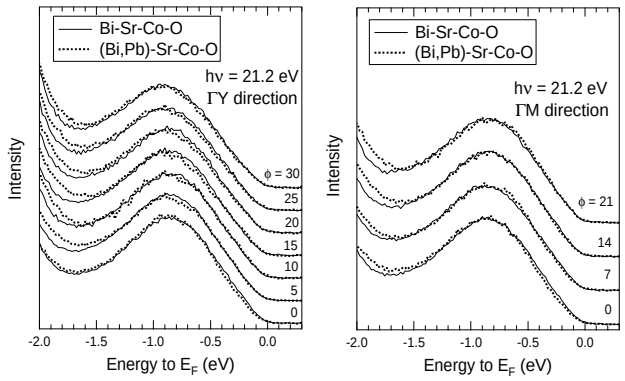

FIG. 9. ARPES spectra of the Bi-Sr-Co-O and (Bi,Pb)-Sr-Co-O samples near the Fermi level along the ΓY and ΓM directions of the (Bi,Pb)SrO_2 layer. The ΓY direction corresponds to the Co-Co direction of the Co-O triangular lattice. ϕ denotes an angle between the sample surface normal and the emission direction of the collected photoelectrons.